Máté Baranyi and Tamás Szabados

Illustration to time series

Contents

List of Figures

1

Illustration

1.1 1D examples

1.1.1 ARMA examples

Example 1.1. Figure 1.1 shows a typical trajectory of a MA(4) process and its prediction based on the finite past $X_0, \dots, X_{n-1}$. The second and third panel show its covariance function and spectral density. The MA polynomial is $\beta(z) = 1 - \frac{1}{2}z + \frac{1}{2}z^2 + \frac{1}{3}z^3 - \frac{1}{3}z^4$. Observe that the covariance is 0 if $h > q = 4$.

The first panel on Figure 1.2 shows the mean square prediction error as a function of n as X_n is predicted. The prediction error goes to 1, which is the non-zero impulse response b_0, since it is a regular process. The last panel shows $\det(\boldsymbol{C}_n)$.

Example 1.2. Figure 1.3 shows a typical trajectory of a MA(∞) process and its prediction based on the finite past $X_0, \dots, X_{n-1}$. The second and third panel show its covariance function and spectral density. The impulse response function is $b_k = 1/(k+1)$ for $k \geq 0$.

The first panel on Figure 1.4 shows the mean square prediction error as a function of n as X_n is predicted . The prediction error goes to 1, which is the non-zero impulse response b_0, since it is a regular process. The last panel shows $\det(\boldsymbol{C}_n)$.

Example 1.3. Figure 1.5 shows a typical trajectory of a sliding summation process and its prediction based on the finite past $X_0, \dots, X_{n-1}$. The second and third panel show its covariance function and spectral density. The parameters are

$$b_k = \begin{cases} 1 & (k = 0) \\ 1/|k| & (k \neq 0) \end{cases} .$$

Observe that $|\log f|$ is significantly larger here than in the case of MA(∞).

The first panel on Figure 1.6 shows the mean square prediction error as a function of n as X_n is predicted. The prediction error decreases. The last panel shows $\det(\boldsymbol{C}_n)$.

Example 1.4. Figure 1.7 shows a typical trajectory of a stable AR(4) process and its prediction based on the finite past $X_0, \dots, X_{n-1}$. The second, third, and fourth panel show its impulse response b_k coefficients, covariance function,

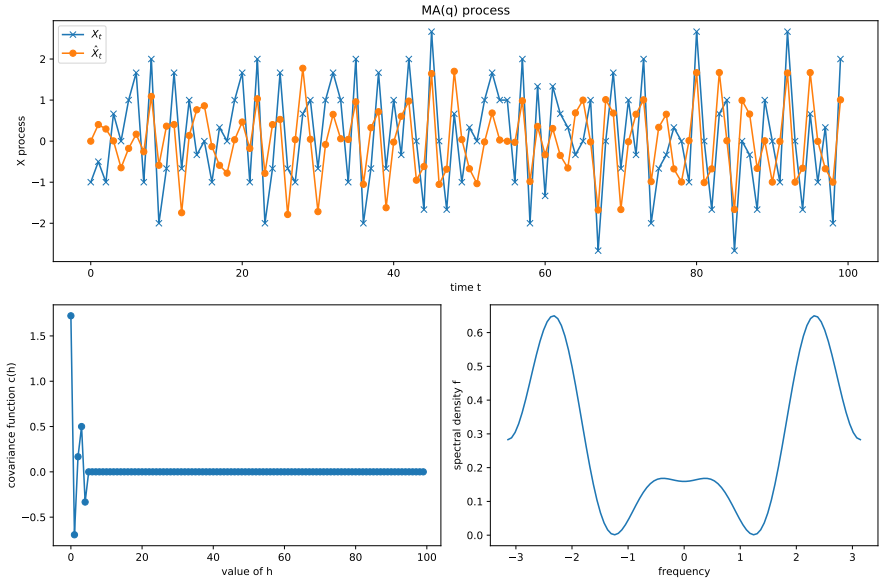

FIGURE 1.1
A typical trajectory and its prediction of an MA(4) process, with its covariance function and spectral density in Example 1.1.

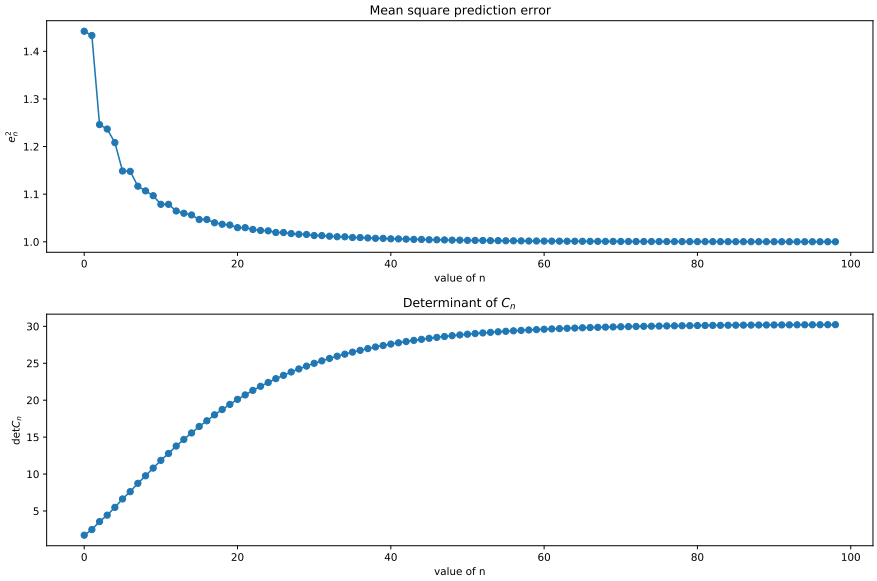

FIGURE 1.2
The mean square prediction error and $\det(\boldsymbol{C}_n)$ of an MA(4) process in Example 1.1.

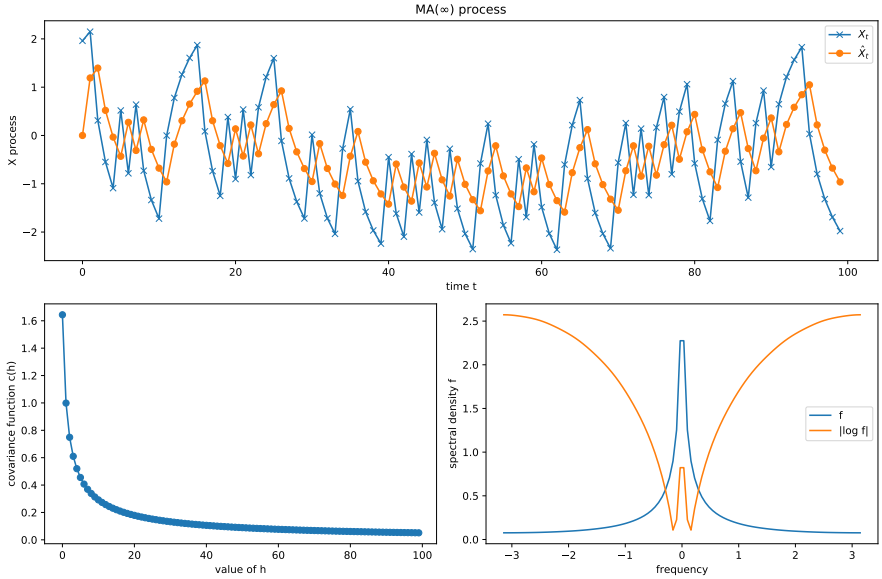

FIGURE 1.3
A typical trajectory and its prediction of an MA(∞) process, with its covariance function and spectral density in Example 1.2.

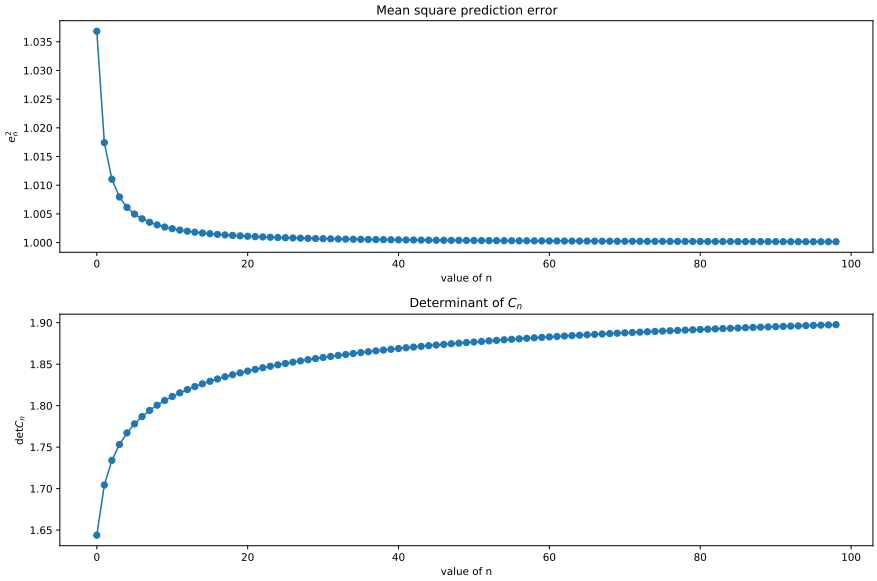

FIGURE 1.4
The mean square prediction error and $\det(\boldsymbol{C}_n)$ of an MA(∞) process in Example 1.2.

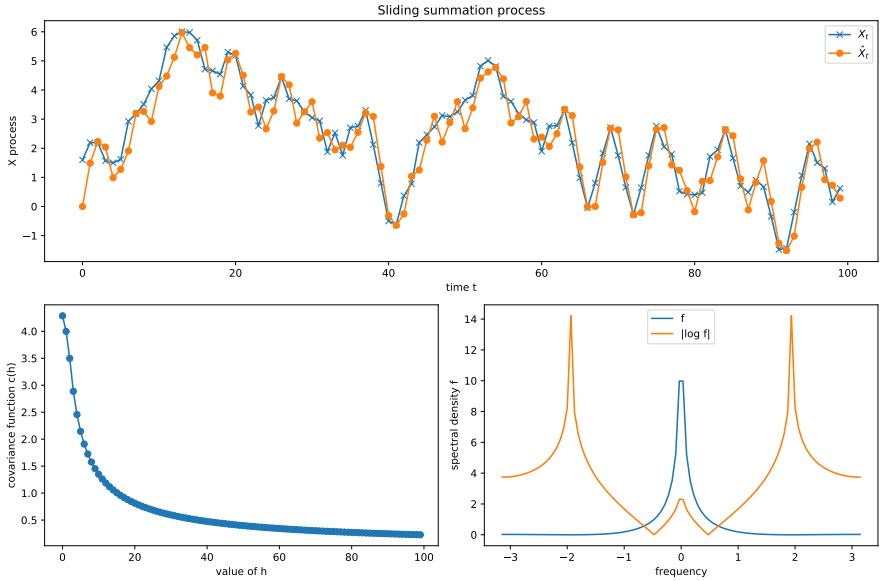

FIGURE 1.5
A typical trajectory and its prediction of a sliding summation process, with its covariance function and spectral density in Example 1.3.

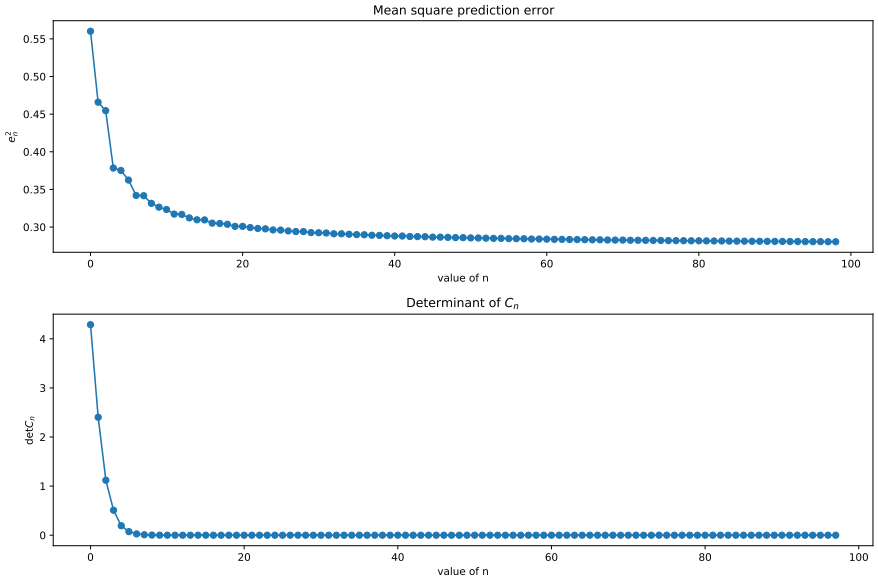

FIGURE 1.6
The mean square prediction error and det($\boldsymbol{C}_n$) of a sliding summation process in Example 1.3.

and spectral density. The AR polynomial is $\alpha(z) = 1 - \frac{7}{6}z + \frac{1}{2}z^2 + \frac{1}{12}z^3 - \frac{1}{12}z^4$ and $\beta = \frac{1}{2}$. The last panel shows the exponential decrease of the covariance function.

The first panel on Figure 1.8 shows the mean square prediction error of this process as a function of n as X_n is predicted. The prediction error goes to 1, which is the non-zero impulse response b_0, since it is a regular process. The last panel shows $\det(\boldsymbol{C}_n)$.

Example 1.5. Figure 1.9 shows a typical trajectory of a stable ARMA$(4, 4)$ process and its prediction based on the finite past $X_0, \ldots, X_{n-1}$, see Subsection **??**. The second, third, and fourth panel show its impulse response b_k coefficients, covariance function, and spectral density. The AR polynomial is $\alpha(z) = 1 - \frac{7}{6}z + \frac{1}{2}z^2 + \frac{1}{12}z^3 - \frac{1}{12}z^4$ and the MA polynomial is $\beta(z) = 1 - \frac{1}{2}z + \frac{1}{2}z^2 + \frac{1}{3}z^3 - \frac{1}{3}z^4$. The last panel shows the exponential decrease of the covariance function.

The first panel on Figure 1.10 shows the mean square prediction error as a function of n as X_n is predicted. The prediction error goes to 1, which is the non-zero impulse response b_0, since it is a regular process. The last panel shows $\det(\boldsymbol{C}_n)$.

1.1.2 Type (0) singular time series

In the Lebesgue decomposition one can further decompose the singular spectral measure:

$$dF_s = dF_d + dF_c,$$

where dF_d is the discrete spectrum corresponding to at most countable many jumps of the spectral distribution function F, while dF_c is the continuous singular spectrum.

(a) A typical example for a process with discrete spectrum:

$$X_t = \sum_{j=1}^{n} A_j e^{it\omega_j}, \qquad t \in \mathbb{Z}, \tag{1.1}$$

where $-\pi < \omega_1 < \cdots < \omega_n \le \pi$; $A_1, \ldots, A_n$ are uncorrelated random variables with mean 0 and variance s_j^2 $(j = 1, \ldots, n)$. (The A_j's can be e.g. independent Gaussian random variables.)

This process is weakly stationary with

$$c(k) = \mathbb{E}(X_{t+k}\overline{X_t}) = \sum_{j=1}^{n} \mathbb{E}(|A_j|^2)e^{ik\omega_j} = \sum_{j=1}^{n} s_j^2 e^{ik\omega_j} = \int_{\pi}^{\pi} e^{ik\omega}\, dF(\omega)$$

for $k \in \mathbb{Z}$, where

$$F(\omega) = \sum_{\omega_j \le \omega} s_j^2, \qquad \omega \in [-\pi, \pi].$$

Observe that the covariance function does not tend to 0 as $k \to \infty$.

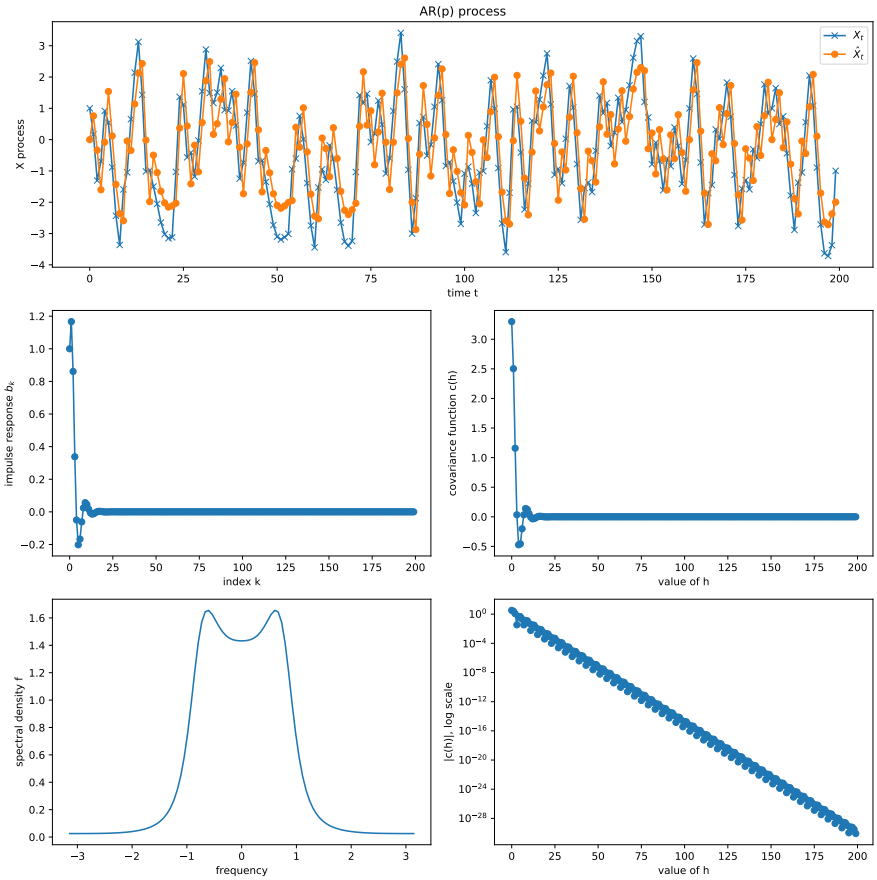

FIGURE 1.7
A typical trajectory and its prediction of a stable AR(4) process, with its b_k coefficients, covariance function, and spectral density in Example 1.4.

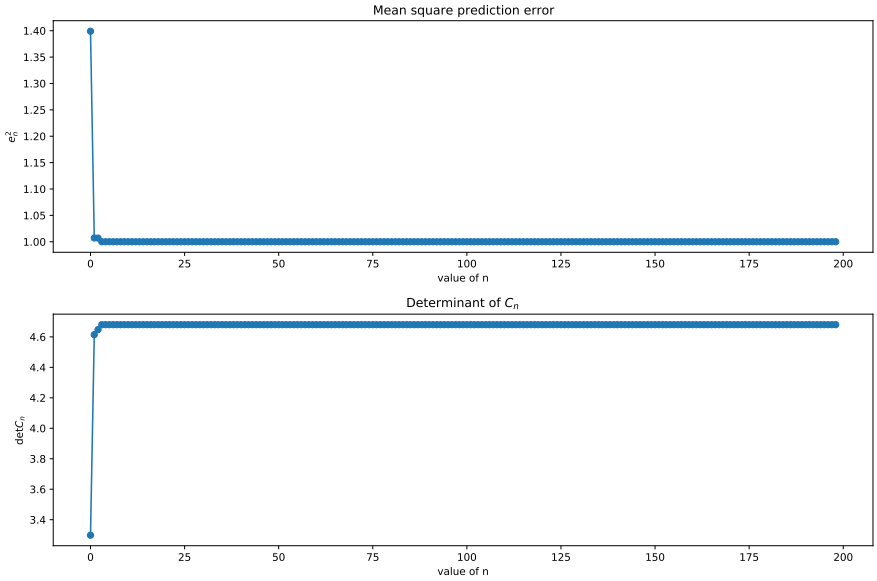

FIGURE 1.8
The mean square prediction error and det($\boldsymbol{C}_n$) of a stable AR(4) process in Example 1.4.

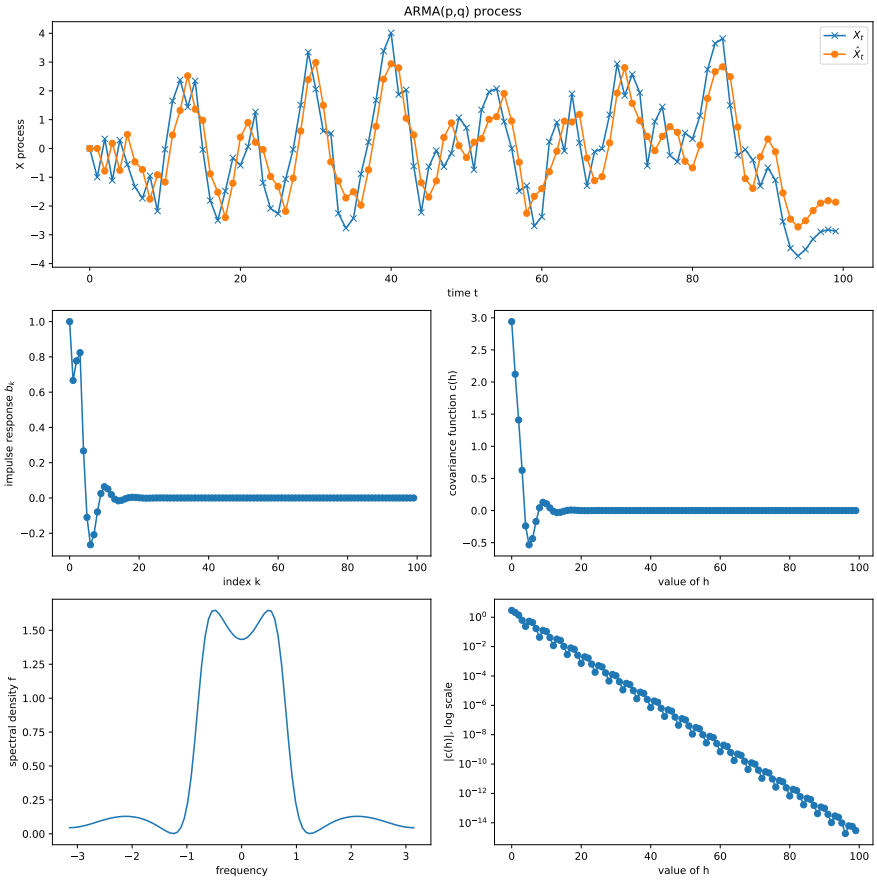

FIGURE 1.9
A typical trajectory and its prediction of a stable ARMA(4,4) process, with its b_k coefficients, covariance function, and spectral density in Example 1.5.

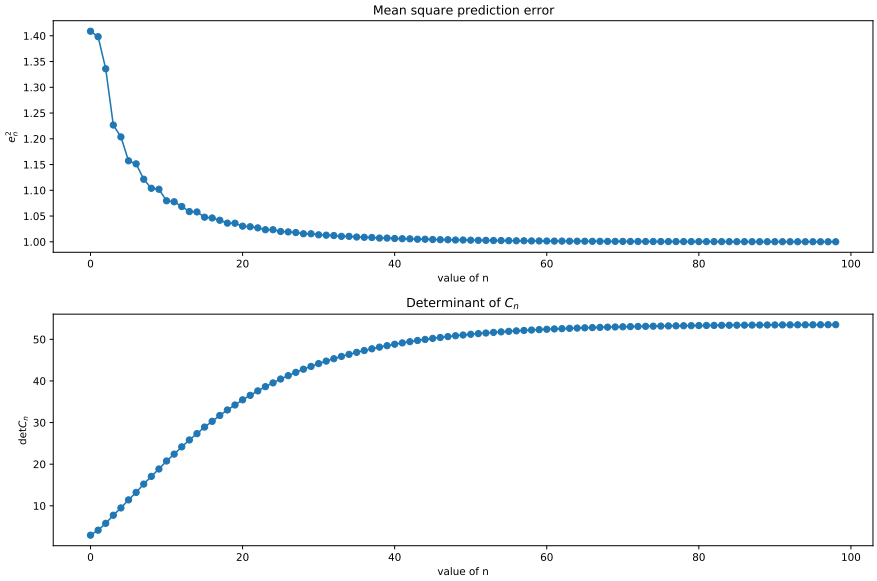

FIGURE 1.10
The mean square prediction error and $\det(\boldsymbol{C}_n)$ of an ARMA(p, q) process in Example 1.5.

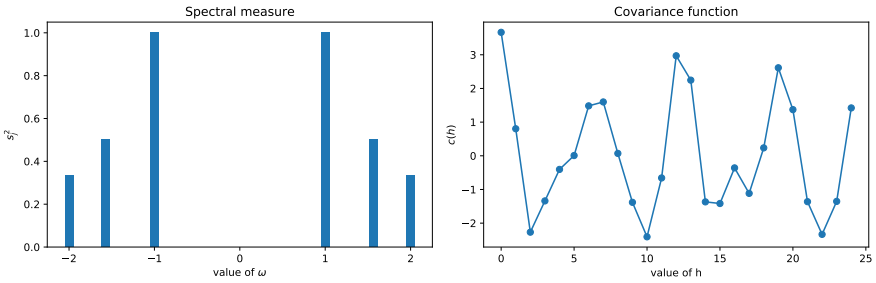

FIGURE 1.11
Spectral measure and covariance function of a Type(0) singular process in Example 1.6.

Example 1.6. Figure 1.11 shows the spectral measure and the covariance function of a Type (0) process (1.1) with $n = 6$. The frequencies ω_j are $\{-2, -\pi/2, -1, 1, \pi/2, 2\}$ and the variances s_j^2 are $\{1, 1/2, 1/3, 1/3, 1/2, 1\}$. Since the spectral measure is

The first panel on Figure 1.12 shows the mean square prediction error e_n^2 when predicting X_n based on the finite past $X_0, \ldots, X_{n-1}$. If $n \geq 5$, square error $e_n^2 = 0$. On the second panel $\det(\boldsymbol{C}_n)$ is shown, which is also 0 if $n \geq 6$.

(b) The standard example for a continuous singular function on $[0, 1]$ is the Cantor function γ, 'the devil's ladder'. Suppose $\mathcal{C}$ is the Cantor set in $[0, 1]$, that is, $x \in \mathcal{C}$ if and only if in base 3 expansion,

$$x = \sum_{n=1}^{\infty} a_n 3^{-n}, \quad a_n = 0 \text{ or } 2.$$

Then the Cantor function $\gamma : [0, 1] \to [0, 1]$ can be defined as

$$\gamma(x) = \begin{cases} \sum_{n=1}^{\infty} \frac{1}{2} a_n 2^{-n}, & x = \sum_{n=1}^{\infty} a_n 3^{-n} \in \mathcal{C}; \\ \sup\{\gamma(y) : y \leq x,\ y \in \mathcal{C}\}, & x \in [0, 1] \setminus \mathcal{C}. \end{cases}$$

Then $\gamma(0) = 0$, $\gamma(1) = 1$, γ is non-decreasing on $[0, 1]$, and $\gamma'(x) = 0$ for a.e. $x \in [0, 1]$.

By the case $d = 1$ of Corollary **??**, the definition

$$F(\omega) = \gamma\left(\frac{\omega + \pi}{2\pi}\right), \quad \omega \in [-\pi, \pi],$$

gives the spectral distribution function of a singular stationary time series X. Heuristically, the spectrum of X consists of the points of an uncountable but zero Lebesgue measure Cantor set, with infinitesimally small amplitudes.

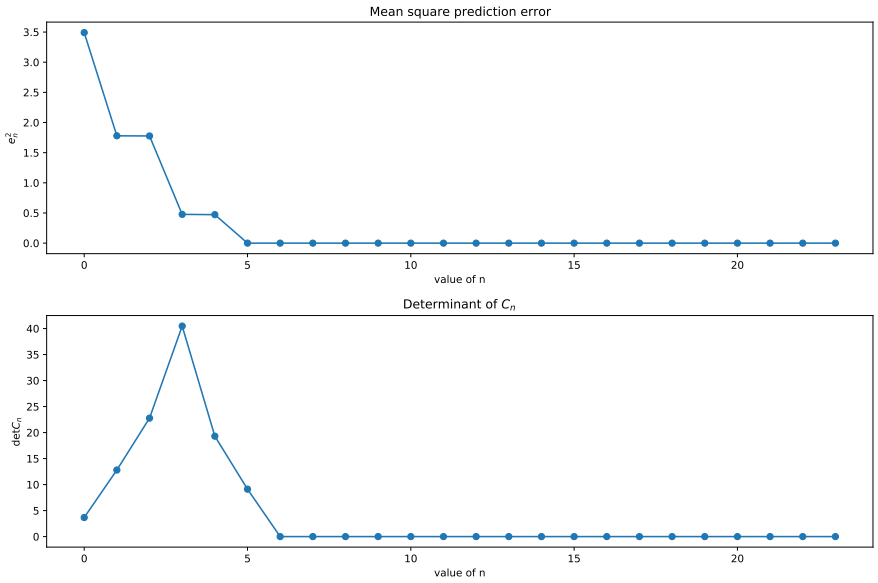

FIGURE 1.12
Prediction error and $\det(\boldsymbol{C}_n)$ of a Type(0) singular process in Example 1.6.

1.1.3 Type (1) singular time series

A simple example for a singular time series corresponding to case (1) of Theorem **??** is the one with spectral density function

$$f(\omega) = \begin{cases} \frac{1}{2}, & |\omega| \le 1; \\ 0, & 1 < |\omega| \le \pi. \end{cases}$$

By the case $d = 1$ of a Corollary, one can construct a singular stationary time series with this spectral density.

Its covariance function is

$$c(k) = \int_{-1}^{1} e^{ik\omega} \frac{1}{2} d\omega = \begin{cases} 1, & k = 0; \\ \frac{\sin k}{k}, & k \neq 0. \end{cases}$$

It is an example for an absolutely non-summable covariance function which still corresponds to an absolutely continuous spectral measure. On the other hand, $\sum_k c(k)$ converges conditionally; also, $\sum_k |c(k)|^2 < \infty$.

Generalizing the previous example, observe the following interesting phenomenon. For any $\delta > 0$ fixed, a time series with spectral density

$$f(\omega) = \begin{cases} \frac{1}{2(\pi-\delta)}, & |\omega| \le \pi - \delta; \\ 0, & \pi - \delta < |\omega| \le \pi. \end{cases}$$

is still singular, like the one above. On the other hand, if we take $\delta = 0$, that

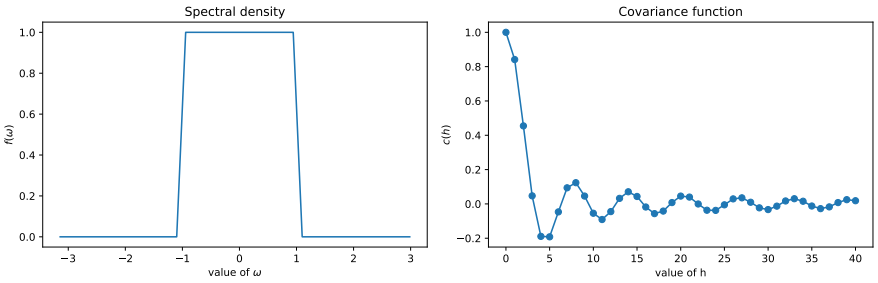

FIGURE 1.13
Spectral density and covariance function of a Type (1) singular process in Example 1.7.

is, $f(\omega) = \frac{1}{2\pi}$ for any $\omega \in [-\pi, \pi]$, then the time series becomes a regular, orthonormal series.

Example 1.7. Figure 1.13 shows the spectral density and the covariance function of the above described Type (1) singular process.

The first panel on Figure 1.14 shows the mean square prediction error e_n^2 when predicting X_n based on the finite past $X_0, \ldots, X_{n-1}$. As n is growing, the prediction error is going to 0, since this is a singular process. On the second panel $\det(\boldsymbol{C}_n)$ is shown, which goes to 0 as well

1.1.4 Type (2) singular time series

An example for case (2) of a Theorem is the following spectral density:

$$f(\omega) = e^{-\frac{1}{|\omega|}}, \quad \omega \in [-\pi, \pi] \setminus \{0\}, \quad f(0) = 0.$$

Then $f(\omega) > 0$ a.e. and f is continuous everywhere on $[-\pi, \pi]$,

$$\int_{-\pi}^{\pi} f(\omega) d\omega < \infty, \quad \int_{\pi}^{\pi} \log f(\omega) d\omega = \int_{-\pi}^{\pi} -\frac{1}{|\omega|} = -\infty.$$

By the case $d = 1$ of a Corollary, one can construct a singular stationary time series $\{X_t\}$ with this spectral density. A Theorem later shows that a time series can be represented as a two-sided infinite MA (a sliding summation) if and only if it has constant rank, that is, in 1D its spectral density is positive a.e., like in the case of this $\{X_t\}$. However, since this $\{X_t\}$ is singular, it cannot be represented as a causal (one-sided) infinite MA. In general, in 1D the same is true for any singular time series of Type (2) and only for these ones.

Example 1.8. Figure 1.15 shows the spectral density and the covariance function of the above described Type (2) singular process. The last few values

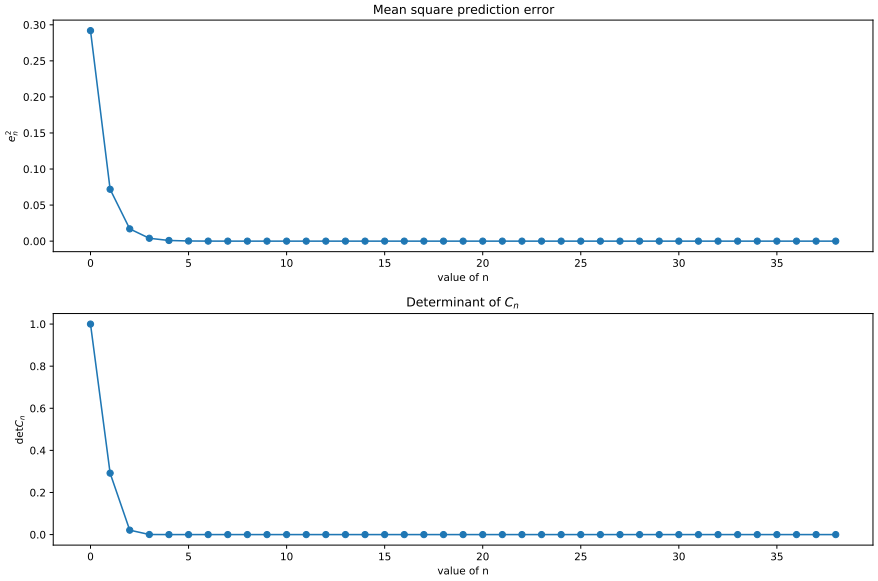

FIGURE 1.14
Prediction error and $\det(\boldsymbol{C}_n)$ of a Type (1) singular process in Example 1.7.

of $c(h)$ are not used because of the numerical distortion of the IDFT (FFT) procedure used to compute the covariance function from the spectral density.

The first panel on Figure 1.16 shows the mean square prediction error e_n^2 when predicting X_n based on the finite past $X_0, \ldots, X_{n-1}$. As n is growing, the mean square prediction error is eventually going to 0, since this is a singular process. The second panel shows $\det(\boldsymbol{C}_n)$, which goes to 0 as well.

1.2 Multi-D example

Example 1.9. Figure 1.17 shows typical trajectories of a 3D VAR(2) process, together with its impulse response functions and covariance functions. Figure 1.18 shows the spectral densities. The parameters are $\boldsymbol{\beta} = \boldsymbol{I}_3$, $\boldsymbol{\alpha}_0 = \boldsymbol{I}_3$,

$$\boldsymbol{\alpha}_1 = \begin{bmatrix} -1 & 0 & 0 \\ 1/2 & -4/5 & 0 \\ -1/2 & 1/3 & -1/6 \end{bmatrix}, \qquad \boldsymbol{\alpha}_2 = \begin{bmatrix} 1/2 & 0 & 0 \\ 1/3 & 1/5 & 0 \\ -1/2 & 1 & -1/6 \end{bmatrix}.$$

The third panel of Figure 1.17 shows that the off-diagonal entries of the matrix $\boldsymbol{H}_k$ are 0. The first of Figure 1.18 show that the spectral densities of the

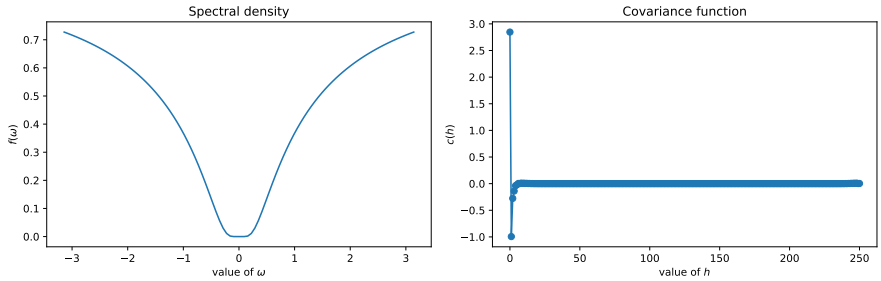

FIGURE 1.15
Spectral density and covariance function of a Type (2) singular process in Example 1.8.

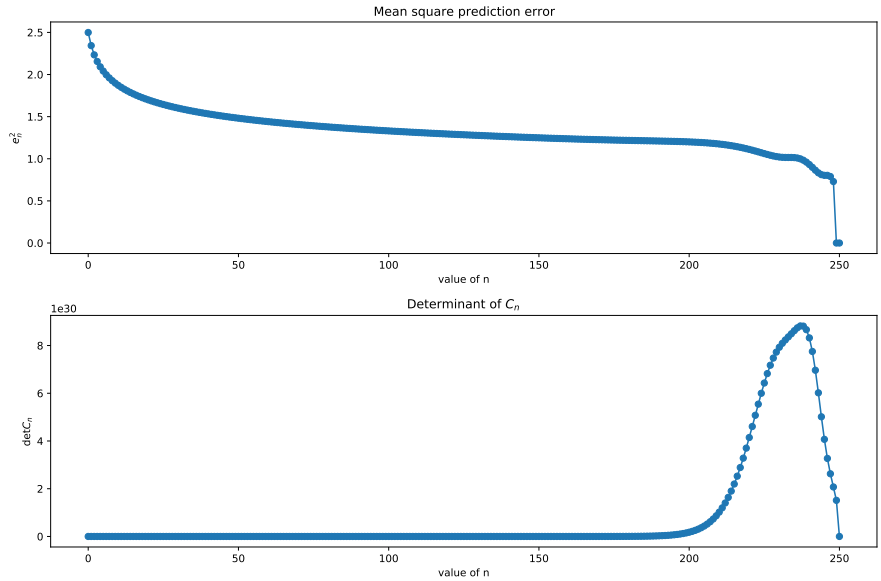

FIGURE 1.16
Prediction error and $\det(\boldsymbol{C}_n)$ of a Type (2) singular process in Example 1.8.

diagonal entries are even functions, similarly the real parts of the off-diagonal entries, while the imaginary parts of the off-diagonal entries are odd functions.

1.3 Real word example

Example 1.10. The previously detailed low-rank approximation is illustrated on a financial dataset containing stock exchange log-returns: Istanbul stock exchange national 100 index, S&P 500 return index, stock market return index of Germany, UK, Japan, Brazil, the MSCI European index, and the MSCI emerging markets index; ranging from June 5, 2009 to February 22, 2011. It is a $d = 8$ dimensional time series dataset of length $n = 535$.

In Figure 1.19, the eigenvalue processes of the estimated M_j matrices are shown in the frequency domain. Based on this, the time series is of rank approximately 3, thus we can apply the outlined low-rank approximation with $m = 3$. In Figure 1.20, the individual variables of the original data and its rank 3 approximation are illustrated. There are calculated root mean square error (RMSE) values under each subplot. The 3 leading PC's, back-transformed to the time domain, are to be found in Figure 1.21.

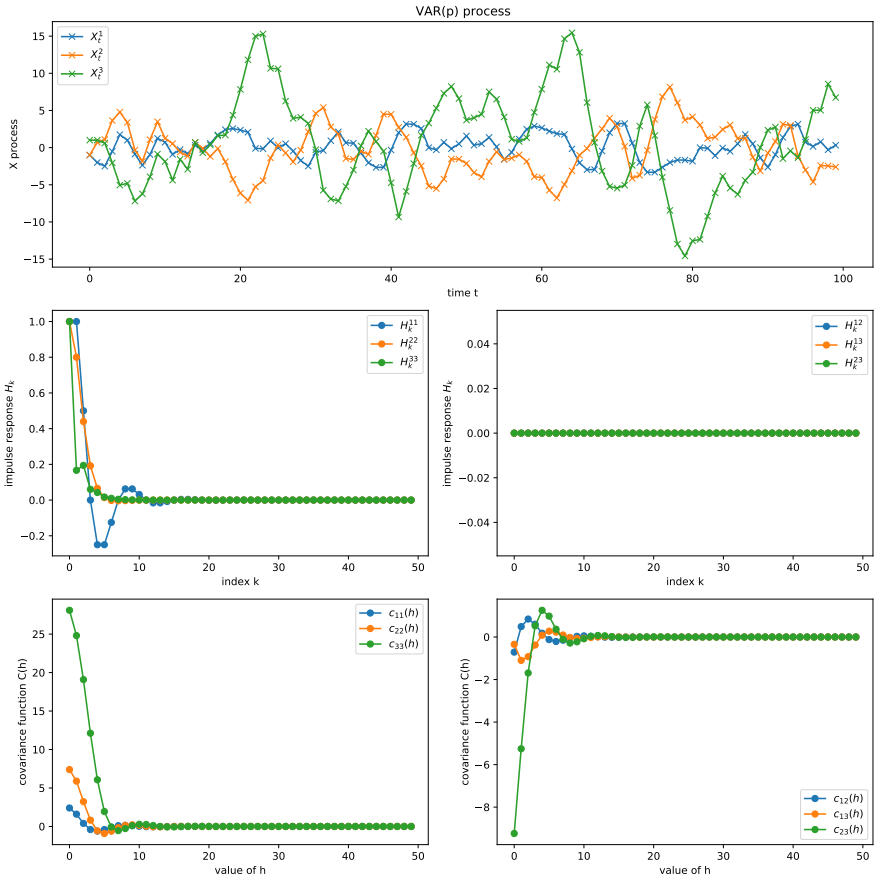

FIGURE 1.17
Typical trajectories of a 3D VAR(2) process, with its impulse response functions and covariance functions in Example 1.9.

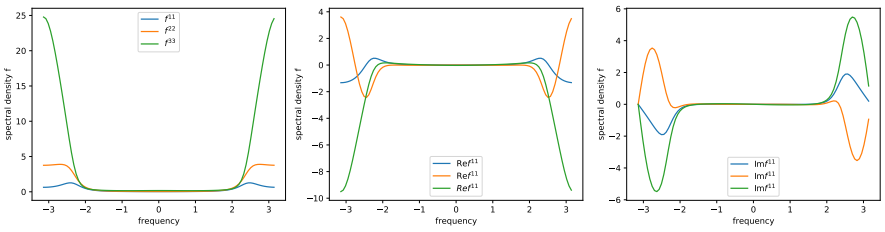

FIGURE 1.18
Spectral densities in Example 1.9.

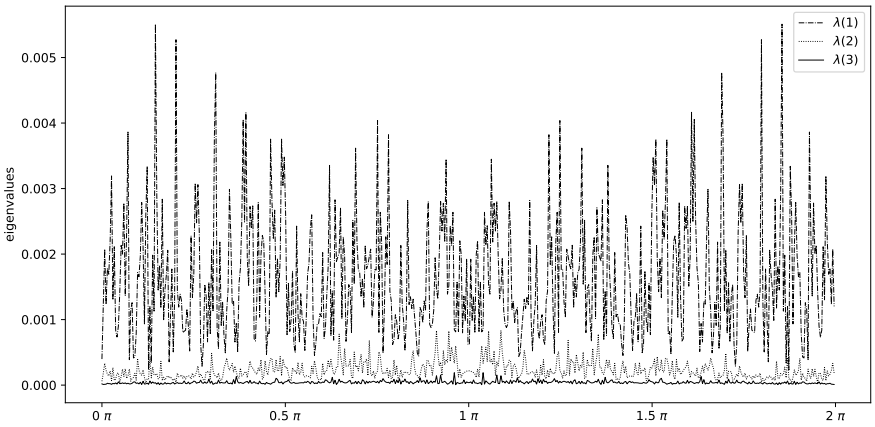

FIGURE 1.19
Eigenvalue processes of the estimated $\boldsymbol{M}_j$ $(j = 0, \ldots, 534)$ matrices over $[0, 2\pi]$, ordered decreasingly in Example 1.10.

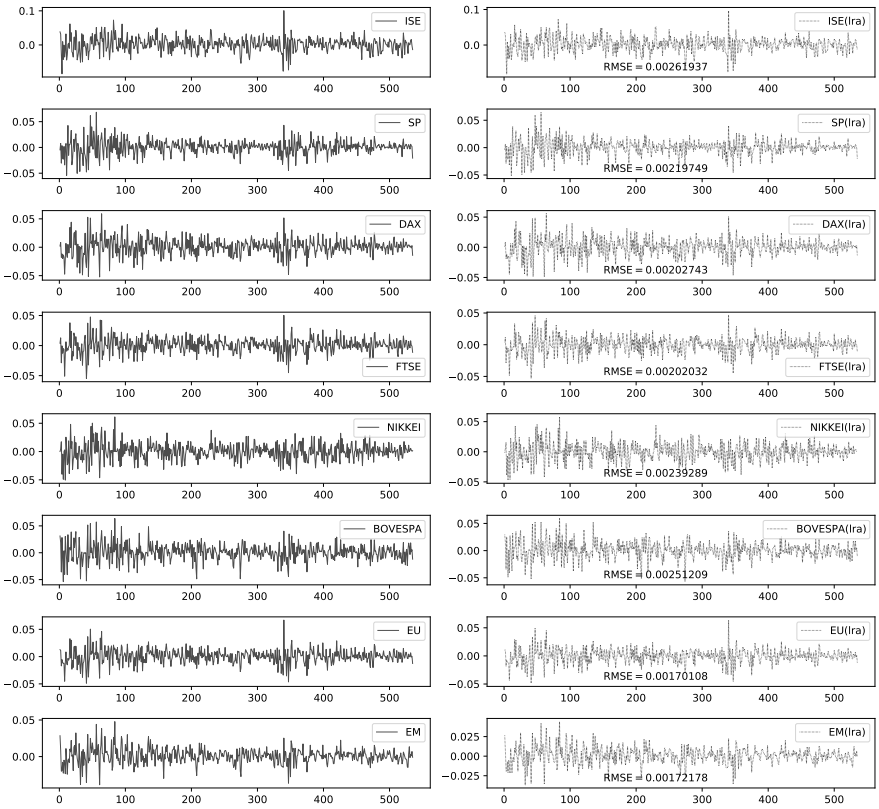

FIGURE 1.20
Approximation of the original time series by a rank 3 time series in Example 1.10.

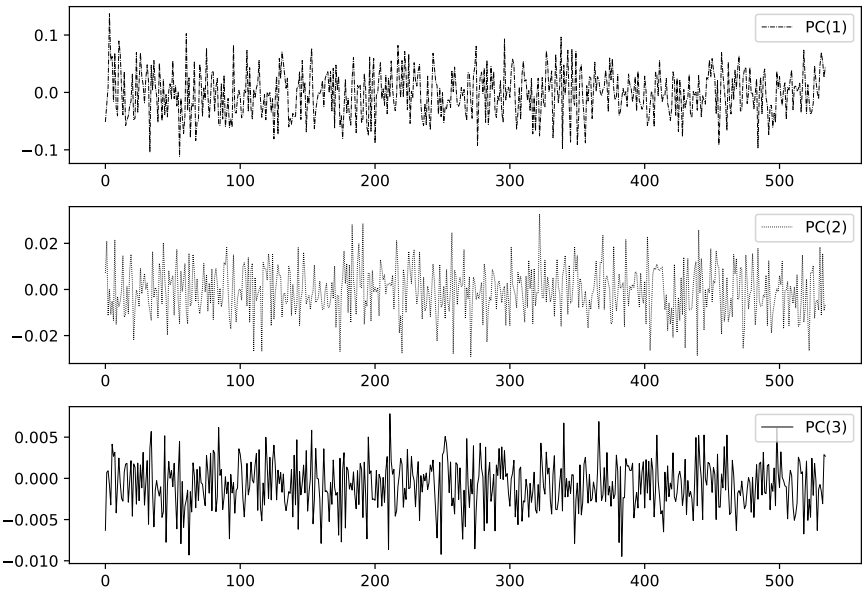

FIGURE 1.21
The 3 leading PC's of the stock exchange data in the time domain in Example 1.10.